

# Actuation Models and Dissipative Control in Empirical Galerkin Models of Fluid Flows

Bernd R. Noack

Gilead Tadmor

Marek Morzyński

Hermann-Föttinger-Institute  
 of Fluid Mechanics  
 Technical University of Berlin  
 Straße des 17 Juni 135  
 D-10623 Berlin, Germany  
 noackbr@pi.tu-berlin.de

Electrical & Computer  
 Engineering Department  
 Northeastern University  
 440 Dana Research Building  
 Boston, MA 02115, U.S.A.  
 tadmor@ece.neu.edu

Inst. Combustion Engines &  
 Basics of Machine Design  
 Poznań University of Technology  
 ul. Piotrowo 3  
 PL 60-965 Poznań, Poland  
 marek.morzynski@put.poznan.pl

**Abstract**— A representation of actuation effects is developed for low-order empirical Galerkin models of incompressible fluid flows. These actuation models fill a missing link and, indeed, provide a key enabler towards feedback design in flow control utilizing empirical Galerkin models. A flow control strategy is proposed based on the extended flow models and on the design of dissipative feedback control. This strategy is successfully applied to benchmark flow control problems involving vortex shedding behind a circular cylinder.

## I. INTRODUCTION

This proof-of-concept study concerns feedback flow control design with empirical Galerkin models. Feedback control is increasingly realized as a key enabler for stretching the dynamic range of operating conditions in aerodynamic applications. Examples are mixing and combustion control in engine combustors (e.g. screech prevention) and separation control for aggressive maneuvers of air vehicles.

Feedback design begins with a choice of the number, location and basic characteristics of actuators and sensors. The exploration of good actuation and sensing solutions and eventual control design are prohibitively expensive with computational fluid dynamics (CFD) models. Low-dimensional flow models are therefore sought as practical enablers.

An efficient path to low-dimensional flow models is offered by the empirical Galerkin method based on a Karhunen-Loève decomposition of flow data [1] — also known as proper orthogonal decomposition (POD). Utilizing the low-order empirical Galerkin ansatz as a viable framework for design-oriented models requires the ability to predict actuation effects. The implementation of actuation effects in empirical Galerkin models faces two principal challenges. First, the actuation changes the flow, thus possibly requiring a reshaping of the dominant expansion modes. Secondly, the effect of actuation must be explicitly modeled as free input, i.e. the actuation frequency and amplitude must not be hardwired in the Karhunen-Loève modes.

The ubiquitous cylinder wake flow is used here to illustrate the problem. It has been considered under a variety of actuation mechanisms, including volume forces [2], cylinder motion [3], local synthetic jets and zero-net-flow source / sink actuators [4], [5]. So far, only few Galerkin models of controlled vortex shedding have been proposed [6]. Promising Galerkin approaches have been developed for near-wall actuation, including, e.g., a volume force implemented in an 8-dimensional model for skin-friction reduction [7] and a framework for the near-wall effect of the acoustic actuator [8].

In the present study, the hardwiring between wall and flow unsteadiness is removed by the incorporation of additional *dynamic actuation modes* in the Galerkin expansion. The amplitudes of these actuation modes are free actuation inputs, whereupon the dynamics

of remaining modified Karhunen-Loève modes are derived in a Galerkin projection on the Navier-Stokes equation. The inclusion of the actuation modes in the Galerkin approximation is therefore a new and important aspect, addressing a well recognized gap in existing POD modeling practice that was inhibitive for the use of such models for control design. In §II, the corresponding mathematical framework for actuation effects is elaborated. In §III, this framework is applied to the actuated cylinder wake.

## II. ACTUATION EFFECTS IN EMPIRICAL GALERKIN MODELS

The incorporation of actuation effects in empirical Galerkin models of incompressible flows in steady domains is discussed in this section. In §II-A, the standard approach [1] is shown to hardwire the actuation and flow structure. In §II-B, a non-equilibrium model of [9] is briefly recapitulated, which has turned out to be a crucial enabler for capturing flow control transients. In §II-C, the volume force is incorporated. In §II-D, the concept of dynamic actuation modes is introduced to separate imposed flow unsteadiness and the coherent-structure response of the flow. In §II-E, the unsteady body motion is shown to be resolved by a combination of a volume force and of an actuation mode.

### A. Standard modeling approach

Empirical Galerkin models are based on experimental flow data or on a direct numerical simulation. This simulation approximates a solution of the non-dimensionalized, incompressible Navier-Stokes equation

$$\partial_t \mathbf{u} + \nabla \cdot (\mathbf{u}\mathbf{u}) = -\nabla p + \frac{1}{Re} \Delta \mathbf{u}, \quad (1)$$

where  $\mathbf{x}$  represents the location,  $t$  the time,  $\mathbf{u}$  the velocity and  $p$  the pressure. The Reynolds number  $Re = UD/\nu$  is the order parameter and based on scales used for the non-dimensionalization, i.e. the velocity scale  $U$ , length scale  $D$  and the kinematic viscosity of the fluid  $\nu$ . The equation of continuity is expressed by

$$\nabla \cdot \mathbf{u} = 0. \quad (2)$$

The flow domain  $\Omega$  is assumed to be steady and velocity fields are embedded in the Hilbert space of square-integrable vector fields  $\mathcal{L}_2(\Omega)$  with the inner product

$$(\mathbf{u}, \mathbf{v})_\Omega := \int_\Omega dV \mathbf{u} \cdot \mathbf{v}, \quad \mathbf{u}, \mathbf{v} \in \mathcal{L}_2(\Omega). \quad (3)$$

The Galerkin approximation of the flow is expressed by

$$\mathbf{u}^{[N]} = \sum_{i=0}^N a_i(t) \mathbf{u}_i(\mathbf{x}), \quad (4)$$

where  $\mathbf{u}_0$  represents the time-averaged field and  $\mathbf{u}_i$ ,  $i = 1, \dots, N$ , are Karhunen-Loève modes, which form an orthonormal set with respect to the inner product (3). Time dependency is described by the Fourier coefficients  $a_i$ . Following a notation of Rempfer [10],  $a_0 \equiv 1$  by definition. In the snapshot method [1], the Karhunen-Loève modes  $\mathbf{u}_i$  are constructed as linear combinations of fluctuation snapshots  $\mathbf{u}^m - \mathbf{u}_0$ ,  $m = 1, \dots, M$ ,  $M \geq N$ . The chosen combinations minimize the averaged energy residual of the Galerkin ansatz (4) with respect to the snapshot ensemble.

The Galerkin projection of the Galerkin ansatz (4) onto the Navier-Stokes equation (1) yields a system of ordinary differential equations [1],

$$\frac{d}{dt} a_i = \frac{1}{Re} \sum_{j=0}^N l_{ij} a_j + \sum_{j,k=0}^N q_{ijk} a_j a_k \quad \text{for } i = 1, \dots, N, \quad (5)$$

where the linear and quadratic terms represent the viscous and convective Navier-Stokes terms, respectively, with constant coefficients  $l_{ij} := (\mathbf{u}_i, \Delta \mathbf{u}_j)_{\Omega}$ ,  $q_{ijk} := (\mathbf{u}_i, \nabla \cdot (\mathbf{u}_j \mathbf{u}_k))_{\Omega}$ . The pressure term may change the coefficients  $q_{ijk}$ , but not the form (5) [11].

The Navier-Stokes simulation and the corresponding Galerkin model may describe a natural or forced flow. Forcing may, in fact, enhance certain coherent structures and thus help to reduce the dimension of the Galerkin model. Examples are the 4-dimensional model of Kelvin-Helmholtz vortices of a shear-layer [11] excited by periodic inlet condition and the 32-dimensional model of a transitional boundary layer manipulated by a periodic tripping wire upstream the observation region considered for the Galerkin model [10]. Obviously, the chosen Galerkin approximation (4) and the Galerkin system (5) can — at best — reproduce that simulation and cannot describe the flow at other forcing amplitudes or at other frequencies. The Galerkin approximation is hardwired to that actuation and the Galerkin system has no free actuation input. This excludes the standard Galerkin modeling approach for control design.

### B. Shift-mode

As a non-equilibrium model for transient flow, the authors have elaborated the need for a shift-mode in [6], [9]. This shift-mode  $\mathbf{u}_{\Delta}$  is the orthonormalized mean-field correction and is aligned with the difference between the unstable steady Navier-Stokes solution  $\mathbf{u}_s$  and the time-averaged flow  $\mathbf{u}_0$ . Formally, the shift-mode  $\mathbf{u}_{\Delta}$  and its amplitude  $a_{\Delta}$  can be considered as the  $N + 1$ -st mode and Fourier coefficient, respectively.

### C. Volume force

A volume force on the fluid flow may physically represent, for instance, a Lorentz force in magneto-hydrodynamical flows or an external pressure gradient in pipe flows. In this note, the force is assumed to be of the form  $\epsilon \mathbf{g}$  with a time-dependent amplitude  $\epsilon(t)$  and a location-dependent field  $\mathbf{g}(\mathbf{x})$ . This force has to be added on the right-hand side of the Navier-Stokes equation (1) and leads to a forcing term of the form  $\epsilon g_i$  on the right-hand side of the  $i$ -th Galerkin system equation (5). The coefficient  $g_i := (\mathbf{u}_i, \mathbf{g})_{\Omega}$  is time-independent. This simple type of actuation is already elaborated in text books and is included here for reasons of completeness and nomenclature. Evidently, the volume force modifies only the Galerkin system and is a free actuation input.

### D. Wall-imposed flow unsteadiness

The flow may be actuated by a flow unsteadiness at the boundary of the domain  $\partial\Omega$ . Examples are blowing and suction at the wall, an acoustic actuator, or a transverse wall motion. This unsteadiness

is prescribed by a Dirichlet boundary condition for the velocity. In order to distinguish between the imposed unsteadiness and the flow response, the velocity field is decomposed as

$$\mathbf{u} = \mathbf{u}_0 + \tilde{\mathbf{u}} + \mathbf{u}^*, \quad (6)$$

where  $\mathbf{u}_0$  represents the time-averaged flow satisfying the time-averaged boundary condition,  $\tilde{\mathbf{u}}$  represents an incompressible velocity field such that  $\mathbf{u}_0 + \tilde{\mathbf{u}}$  fulfills the instantaneous boundary condition, and  $\mathbf{u}^*$  is considered as the fluctuation which fulfills the homogenized boundary condition. The imposed unsteadiness  $\tilde{\mathbf{u}}$  is a design parameter. Its development may be guided by physical intuition.

For reasons of simplicity, the imposed unsteadiness is assumed to be of the form

$$\tilde{\mathbf{u}} = a_c(t) \mathbf{u}_c(\mathbf{x}), \quad (7)$$

where the normalized field  $\mathbf{u}_c(\mathbf{x})$  is called an *actuation mode* and  $a_c$  is the actuation amplitude. Formally, the actuation mode and its amplitude can be included as the mode  $i = -1$  in the Galerkin approximation (4)

$$\mathbf{u}^{[N]} = \sum_{i=-1}^N a_i(t) \mathbf{u}_i(\mathbf{x}), \quad (8)$$

where  $a_{-1} := a_c$ ,  $\mathbf{u}_{-1} := \mathbf{u}_c$ . In (8), the Karhunen-Loève modes minimize the energy residual of the approximation  $\mathbf{u}^* = \mathbf{u} - \mathbf{u}_0 - a_{-1} \mathbf{u}_{-1} \approx \sum_{i=1}^N a_i(t) \mathbf{u}_i(\mathbf{x})$ . These modes are different from the standard Karhunen-Loève modes which incorporate parts of the imposed unsteadiness. In the original ansatz (4), the coefficients  $a_i$ ,  $i = 1, 2, \dots, N$  cannot be chosen independently of the unsteady boundary condition for the velocity field. In contrast, the generalized Galerkin approximation (8) completely absorbs the unsteady Dirichlet condition in  $a_{-1}$  and allows any arbitrary choice of the Fourier coefficients  $a_i$ ,  $i = 1, 2, \dots, N$  to be consistent with the boundary condition.

The evolution equation of the Fourier coefficients is obtained via the Galerkin projection of (8) onto (1),

$$\frac{d}{dt} a_i = f_i \frac{d}{dt} a_{-1} + \frac{1}{Re} \sum_{j=-1}^N l_{ij} a_j + \sum_{j,k=-1}^N q_{ijk} a_j a_k \quad (9)$$

for  $i = 1, 2, \dots, N$  with  $f_i := -(\mathbf{u}_i, \mathbf{u}_{-1})_{\Omega}$ . Thus, the actuation input  $a_{-1}$  enters the right-hand side of the generalized Galerkin system (9), in form of a first derivative, a linear term, and in the products with the free  $a_i$ ,  $i = 1, 2, \dots, N$ .

### E. Unsteady cylinder motion

The proposed Galerkin method for volume and boundary actuation can easily be generalized for several forces or for several wall actuators including combinations thereof. In this section, only one combination for a transversely moving circular cylinder in uniform free-stream is considered.

Let  $x, y$  be a Cartesian coordinate system where the flow is aligned with the  $x$ -direction. Without loss of generality, the center of the transversely moving cylinder shall be described by  $[0, Y]$  in a laboratory frame of reference. In a body-fixed frame of reference, the cylinder is at the origin  $[0, 0]$  and the free-stream has a  $y$ -component  $v = -dY/dt$ . This imposed free-stream unsteadiness shall be described by an actuation mode  $\mathbf{u}_{-1}$  which vanishes on the cylinder and converges to  $\mathbf{u} = [0, 1]$  away from the cylinder. The actuation mode is chosen to be the rotated basic mode of a

mathematical Galerkin model [12]. The actuation mode thus essentially represents the transverse potential flow with a thick boundary-layer at the cylinder. The boundary-layer thickness corresponds to the parameters of the basic mode at  $Re = 10$ . This Reynolds number is determined by a typical transverse velocity which is one order of magnitude smaller than the free-stream Reynolds number 100. The Galerkin model is numerically found to be insensitive to the choice of this parameter. The Karhunen-Loève modes absorb a change in the actuation mode by construction (6).

The imposed flow unsteadiness is given by  $\hat{\mathbf{u}} = a_{-1} \mathbf{u}_{-1}$ ,  $a_{-1} = -dY/dt$ . In the cylinder-fixed frame of reference, the acceleration of the cylinder leads to a fictitious volume force  $-d^2Y/dt^2 \mathbf{g}$ ,  $\mathbf{g} = [0, 1]$ , on the right-hand side of the Navier-Stokes equation (1).

Neglecting the cylinder, the actuation mode represents a uniform flow  $\mathbf{u}_{-1} = [0, 1]$  and the Navier-Stokes equation (1) simplifies to  $\partial_t \mathbf{u} = 0$  and  $\partial_t v = da_{-1}/dt = -d^2Y/dt^2$ . In other words, the actuation mode term and the fictitious force annihilate each other. In the current cylinder wake study, this is numerically found to be approximately correct, and the actuation input enters mainly in the linear and quadratic terms.

### III. MODEL-BASED CONTROL OF VORTEX SHEDDING

In this section, the framework outlined in §II is applied to the cylinder for two actuations, a local volume force and a transverse cylinder motion. The focus is placed on ‘least-order’ models which elucidate the main actuation mechanisms.

#### A. The ‘minimal’ Galerkin model of the natural flow

The laminar wake behind a circular cylinder has been studied extensively since about hundred years (see, e.g., the review article [13]). In the current study, the flow is considered at the reference Reynolds number of 100, well above the laminar instability regime’s critical value of 47 [14]. The natural flow is characterized by von Kármán vortex shedding defining a periodic attractor. This attractor and the oscillatory transients leading to the attractor have been described in a reduced-order empirical Galerkin model [9]. This representation is briefly recapitulated here since variants for control are described in the following sections. A detailed discussion of the model and its properties can be found in the original publication.

An energy-resolving model is obtained with the first eight Karhunen-Loève modes which describe the first four shedding harmonics [15]. In fact, already the first pair captures some 96% of the perturbation kinetic energy in the near wake, an ample representation from a control design perspective. However, a Galerkin model which is based on these two modes alone – essentially an ideal oscillator – leads to slowly growing unbounded oscillation amplitudes since it lacks the means to enforce the natural oscillation amplitude. Lacking a dynamic range, this model is therefore unsuitable as a basis for control design. A shift-mode (see §II-B) is a key enabler for covering dynamic properties of the system. This mode captures the energy exchange between the mean flow and the oscillatory modes.

The energy-resolving Galerkin model is reduced to a three-state ‘minimal’ model in [9]. That model is based on the steady Navier-Stokes solution  $\mathbf{u}_s$ , the two leading Karhunen-Loève modes  $\mathbf{u}_i$  and the shift-mode  $\mathbf{u}_\Delta$ . The corresponding Galerkin approximation is given by

$$\mathbf{u} = \mathbf{u}_s + a_1 \mathbf{u}_1 + a_2 \mathbf{u}_2 + a_\Delta \mathbf{u}_\Delta.$$

This ansatz is equivalent to an expansion around the mean flow  $\mathbf{u}_0$  (4) since the mean flow is expressed by  $\mathbf{u}_s + \langle a_\Delta \rangle \mathbf{u}_\Delta$ , the brackets

denoting the time average. However, the expansion around the steady solution simplifies the form of the Galerkin system [9]:

$$\frac{d}{dt} \begin{bmatrix} a_1 \\ a_2 \\ a_\Delta \end{bmatrix} = \begin{bmatrix} \sigma_o & \omega + \gamma a_\Delta & -\beta a_1 \\ -\omega - \gamma a_\Delta & \sigma_o & -\beta a_2 \\ \alpha a_1 & \alpha a_2 & -\sigma_\Delta \end{bmatrix} \begin{bmatrix} a_1 \\ a_2 \\ a_\Delta \end{bmatrix}. \quad (10)$$

Indeed, with the addition of the third shift-mode, this system captures very transparently key ingredients of the wake flow [9]: (i) The instability of the steady flow (represented by the zero state), (ii) the dominant oscillation frequency and its dependence on changes with the mean flow; (iii) the existence of an attractive invariant manifold of transients from the neighborhood of the steady solution to the attractor, and (iv) the stability of a limit cycle attractor. Residual quantitative discrepancies – well expected given the low dimension of (10) – can be resolved, e.g., by invariant manifold methods and the addition of stability modes [9] or by adaptation of the Galerkin coefficients [16].

#### B. Design objectives and constraints

A standard design objective, mentioned above, is the attenuation of vortex shedding dynamics. This objective is motivated by engineering considerations including the reduction of oscillatory forces on ropes in water and on chimneys. Referring to the model (10), this objective means that the amplitude  $r = \sqrt{a_1^2 + a_2^2}$  has to be attenuated.

The following comment concerns critical implications of using the Galerkin model (10) and subsequent actuated variants for control design. Any low order model of a truly distributed and nonlinear system is bound to be restricted to a narrow operating regime for which it is derived. Here, the model was derived primarily for and from the natural vortex shedding regime. The shift-mode enhancement extends this representation to the attractive invariant manifold of transients from the neighborhood of steady flow to the natural vortex shedding oscillations [9]. A key aspect of this model, rooted in the physics of the system, is the natural vortex shedding frequency. If an actuated variant of (10) is to be used for control design, it is therefore essential that the actuated system be maintained within its domain of validity. In particular, it is essential that the basic frequency will remain intact, and that the rate of forced change in the amplitude  $r$  will be (at most) similar to what can be found in natural transients, on which the model is based. Beyond this basic logic, this observation has been supported by both experimental and CFD based analysis, demonstrating the loss of control authority under modified frequency, as well as the accumulated experience in the fluid flow community with failures, when this warning was not heeded.

In summary, the design task that is used as a benchmark in this note is the slow feedback attenuation of the amplitude  $r = \sqrt{a_1^2 + a_2^2}$ , subject to the constraint that actuation maintains the natural vortex shedding frequency. The main purpose of this benchmark is to illustrate the new concept of actuation models as extensions of empirical Galerkin models of fluid flow systems and their use in control design. We therefore do not dwell here on observer design and sensor signal feedback. Those were discussed in [6], [17].

#### C. Actuation model for a volume force

The actuation model for a volume-force actuator is comparatively simple (see §II-C). The control input is the modulation factor denoted by  $\epsilon(t)$ . An important aspect is that this force is assumed to have no effect on the Karhunen-Loève expansion modes in the Galerkin approximation. Consequently, its effect on the Galerkin system is the addition of a linear term  $B \epsilon$ .

In an example considered in [6], actuation is provided by a transversal volume force, supported over a disc in the near-wake as illustrated in Fig. 1. Due to the  $y$ -axis symmetry of the shift mode,

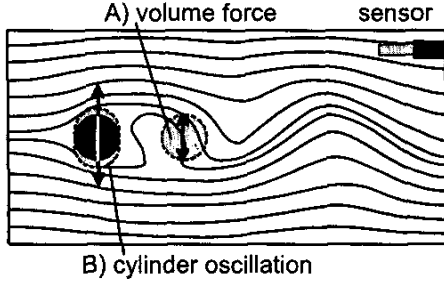


Fig. 1. Principal sketch of the actuated cylinder wake. The cylinder is represented by the black disk. The location of the volume-force actuator (A) is indicated by a grey circle, and the transverse cylinder motion (B) by arrows. Stream-lines represent the natural flow. The figure includes a hot-wire anemometer at a typical experimental position. This sensor has been used in an observer-based control using a Galerkin model [6].

the projection of this volume force on the shift mode vanishes. The inclusion of the volume force amounts therefore to the addition of a term  $B\epsilon = [g_1, g_2, 0]^T \epsilon$  on the right-hand side of (10). Discussions of aspects of control design with this volume force actuation has already been presented in [6], [17] and are therefore left out here.

#### D. Actuation model for an oscillating cylinder

Here, actuation is provided by forced, nearly periodic vertical motion of the cylinder in short strokes (see Fig. 1). In open-loop actuation (used to obtain the vortex shedding POD modes), the transverse motion is prescribed by  $Y = 0.1 \sin \omega t$  (see §II-E). The frequency  $\omega$  is assumed from the natural shedding. This form of actuation was considered in [3]. One modeling challenge, is the moving boundary (i.e., the cylinder) and hence, the boundary conditions in the computation domain. It is therefore convenient to synchronize the spatial frame of reference with the center of the cylinder, whereby the boundary becomes stationary. Consequently, however, the free flow now includes a global sinusoidal vertical component. The necessary changes in the Navier-Stokes equation and its boundary conditions, and the corresponding changes of the Galerkin model were outlined in §II-E.

In the current study, a minimal Galerkin model is constructed for actuated conditions in analogy to the natural flow. The Galerkin approximation is given by an  $N = 2$  truncation of (8) with an added shift- and actuation-mode,

$$\mathbf{u} = \mathbf{u}_s + a_1 \mathbf{u}_1 + a_2 \mathbf{u}_2 + a_\Delta \mathbf{u}_\Delta + a_c \mathbf{u}_c. \quad (11)$$

Figure 2 visualizes the employed modes. Note that the base flow is the steady solution, as in §III-A.

One main consequence is that actuation – represented by  $a_c$  – effects the velocity field itself, whereas the volume force effects only its derivative (i.e. fluid acceleration). To be more specific, the fact that the actuation mode  $\mathbf{u}_c$  is not orthogonal to the oscillation modes means that the expressions for the time derivatives of  $\frac{d}{dt}[a_1, a_2, a_\Delta]$  will include contributions of both  $a_c$  and of its derivative,  $da_c/dt$ , as obtained from the projections in the  $u_1$  and  $u_2$  directions, respectively, of the time derivative of (11). The projection along  $u_\Delta$  vanishes, due to  $y$ -axis symmetry of this mode.

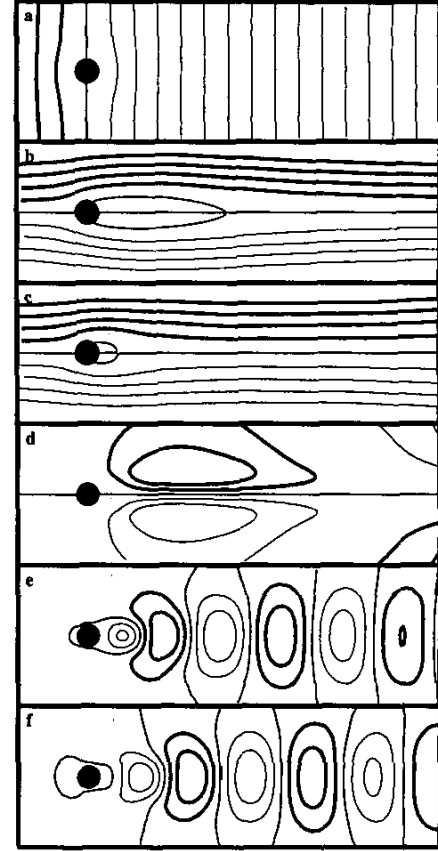


Fig. 2. Galerkin approximation (11). The modes include an actuation representation for the oscillating cylinder and are depicted by stream-lines: (a) The actuation mode, (b) the (unstable) steady flow  $\mathbf{u}_s$ , (c) the natural mean-flow  $\mathbf{u}_0$  (i.e., under vortex shedding), (d) the shift-mode  $\mathbf{u}_\Delta$ , and (e), (f), the Karhunen-Loève modes  $\mathbf{u}_1$  and  $\mathbf{u}_2$ , representing the first vortex shedding harmonic. The plots (c,e,f) were derived from a Karhunen-Loève decomposition of the open-loop actuated cylinder at 0.1D-strokes and at the natural vortex shedding frequency. They are qualitatively very similar to their counterpart for the static cylinder.

A second difference from the volume force case is the contribution of the added term  $d^2 Y/dt^2$  on the right-hand side of the Navier-Stokes equation. The contribution of this transverse field, is again principally captured by  $\mathbf{u}_c$ , and is reflected by a second added term, proportional to  $da_c/dt$ .

The force-units term  $\epsilon = da_c/dt$  is viewed as a control input, in terms of which the system fits into a conventional, pseudo-linear pattern

$$\frac{d}{dt} \mathbf{a} = A(\mathbf{a})\mathbf{a} + B\epsilon \quad (12)$$

where the matrices  $A(\mathbf{a})$  assumes the form

$$A = \begin{bmatrix} \sigma_o & \omega + \gamma a_\Delta & -\beta a_1 + \beta_{c1} a_c & \kappa_1 \\ -\omega - \gamma a_\Delta & \sigma_o & -\beta a_2 + \beta_{c2} a_c & \kappa_2 \\ \alpha a_1 - \alpha_{c1} a_c & \alpha a_2 - \alpha_{c2} a_c & -\sigma_\Delta & \kappa_\Delta + \alpha_{c\Delta} a_c \\ 0 & 0 & 0 & 0 \end{bmatrix} \quad (13)$$

and  $B = [b_1, b_2, 0, 1]^T$ . Numerical parameter values were obtained from a numerical Galerkin projection:  $\sigma_o = 0.0471$ ,  $\sigma_\Delta = 0.0602$ ,  $\omega = 0.9431$ ,  $\gamma = 0.0292$ ,  $\alpha = \beta = 0.0226$ ,  $\alpha_{c1} = \beta_{c1} = 0.0358$ ,

$\alpha_{c2} = \beta_{c2} = 0.206$ ,  $\alpha_{c\Delta} = 0.0110$ ,  $\kappa_1 = -0.7416$ ,  $\kappa_2 = -0.5245$ ,  $\kappa_\Delta = -0.0164$ ,  $b_1 = 0.0558$  and  $b_2 = -0.0182$ . In Fig. 3, the direct numerical simulation, the energy resolving Galerkin model, and the minimal model (12) are compared for the cylinder wake under open-loop actuation. Even the minimal model is seen to approximate well the Navier-Stokes attractor.

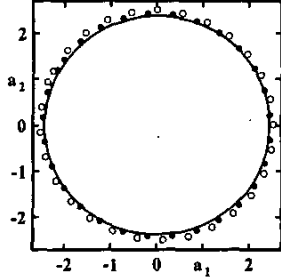


Fig. 3. Galerkin attractor of the wake behind the cylinder transversely oscillating with  $Y = 0.1 \sin \omega t$  at the natural shedding frequency  $\omega$ . The figure displays a phase portrait with the Fourier coefficients of the von Kármán modes  $a_1$ ,  $a_2$  for the simulation (solid line), the energy-resolving Galerkin model ( $\bullet$ ) and the minimal phase-invariant Galerkin model ( $\circ$ ).

#### E. Dissipative control of the oscillating cylinder model

The purpose of design, stated in §III-B, is the slow attenuation of  $\tau$  subject to the constraint that the natural oscillation frequency  $\omega + \gamma a_\Delta$  be left (essentially) intact. The special structure of the system and intended actuation will be utilized to address this task in the nonlinear (12).

The true actuation command in this system is the force applied to the cylinder, or, indeed, the voltage applied to the motor producing that force. Yet, a much simpler setting is used here: As noted earlier, effective actuation of the cylinder wake is restricted to the natural vortex shedding frequency. In this sense, actuation is limited to slow modulation of the phase and amplitude of a periodic motion at the natural frequency. The narrow bandwidth of the closed loop system justifies an instantaneous response assumption — ignoring the actuator's internal dynamics.

Focusing on nearly periodic motion and actuation, it is convenient to move to cylindrical coordinates,  $[a_1, a_2] = [\sin(\phi), \cos(\phi)] r$ , transforming the original system to the form:

$$\frac{d}{dt} r = (\sigma_o - \beta a_\Delta) r + g_r \left( \phi, a_\Delta, a_c, \frac{d}{dt} a_c \right), \quad (14)$$

$$\frac{d}{dt} a_\Delta = -\sigma_D a_\Delta + \beta r^2 + g_\Delta \left( \phi, a_\Delta, a_c, \frac{d}{dt} a_c \right), \quad (15)$$

$$\frac{d}{dt} \phi = \omega + \gamma a_\Delta + \frac{1}{r} g_p \left( \phi, a_\Delta, a_c, \frac{d}{dt} a_c \right), \quad (16)$$

where

$$\begin{aligned} g_r &= \sin(\phi) \left( [\kappa_1 + \beta_{1c} a_\Delta] a_c + b_1 \frac{d}{dt} a_c \right) \\ &\quad + \cos(\phi) \left( [\kappa_2 + \beta_{2c} a_\Delta] a_c + b_2 \frac{d}{dt} a_c \right), \\ g_\Delta &= [\kappa_\Delta + \alpha_{c\Delta} a_c - (\beta_{c1} \sin(\phi) + \beta_{c2} \cos(\phi)) r] a_c, \\ g_p &= \cos(\phi) \left( [\kappa_1 + \beta_{1c} a_\Delta] a_c + b_1 \frac{d}{dt} a_c \right) \\ &\quad - \sin(\phi) \left( [\kappa_2 + \beta_{2c} a_\Delta] a_c + b_2 \frac{d}{dt} a_c \right). \end{aligned}$$

A nearly periodic actuation at the oscillation frequency is of the form

$$a_c = r_c \cos(\phi + \theta_c), \quad \frac{d}{dt} a_c \approx -\frac{d\phi}{dt} r_c \sin(\phi + \theta_c),$$

where the approximation is justified by the fact that  $r_c$  and  $\theta_c$  are slowly varying and  $d\phi/dt$  is represented by the right hand side of (16). In fact, if successful, the proposed control policy will be such that  $d\phi/dt$  could be further approximated by its slowly varying, dominant term,  $\omega + \gamma a_\Delta$ . The purpose of control design is the selection of the slowly varying phase shift  $\theta_c$  and amplitude  $r_c$ .

Denote  $[c_1, c_2] = [\kappa_1 + \beta_{1c} a_\Delta, \kappa_2 + \beta_{2c} a_\Delta]$ . In these terms,

$$g_r = \frac{1}{2} r_c \left[ (c_1 - b_2 \frac{d\phi}{dt}) \sin(2\phi + \theta_c) + (c_2 + b_1 \frac{d\phi}{dt}) \cos(2\phi + \theta_c) - (c_1 + b_2 \frac{d\phi}{dt}) \sin(\theta_c) + (c_2 - b_1 \frac{d\phi}{dt}) \cos(\theta_c) \right]. \quad (17)$$

and

$$g_p = \frac{1}{2} r_c \left[ (c_1 - b_2 \frac{d\phi}{dt}) \cos(2\phi + \theta_c) - (c_2 + b_1 \frac{d\phi}{dt}) \sin(2\phi + \theta_c) + (c_1 + b_2 \frac{d\phi}{dt}) \cos(\theta_c) + (c_2 - b_1 \frac{d\phi}{dt}) \sin(\theta_c) \right]. \quad (18)$$

Each of the terms in (17) and (18) comprises a term involving the second harmonic of  $\phi$  and a slowly varying term. The contribution of the zero-mean, second harmonic terms to the narrow bandwidth dynamics in (14) and (16), is negligible. Considering the contribution of the slowly varying terms, it is noted that the terms multiplying the vector  $[\cos(\theta_c), \sin(\theta_c)]^T$  in (17) and in (18) are mutually orthogonal. The objective to maximize the amplitude of a negative “dc” component of  $g_r$  (for a given stroke amplitude  $r_c$ ) and the constraint requiring to annihilate the “dc” component of  $g_p$ , by the same selection of  $\theta_c$ , are therefore complementary. Thus,  $\theta_c$  has to be selected to achieve the desired alignment

$$\begin{bmatrix} -c_1 - b_2 \frac{d\phi}{dt} \\ c_2 - b_1 \frac{d\phi}{dt} \end{bmatrix} \propto \pm \begin{bmatrix} \sin(\theta_c) \\ \cos(\theta_c) \end{bmatrix}.$$

The minus sign is used here, to serve the goal of attenuating vortex shedding. A plus sign would have been used if amplification were desired. The value of the “dc” component of  $g_r$  is then

$$g_{r0} = -\frac{1}{2} r_c r_m, \quad r_m = \left\| \begin{bmatrix} -c_1 - b_2 \frac{d\phi}{dt} \\ c_2 - b_1 \frac{d\phi}{dt} \end{bmatrix} \right\|.$$

To be effective, the actuation amplitude  $r_c$  must be selected large enough to turn the (averaged) (14) dissipative; e.g.,  $r_c = 2(\rho + \sigma_o - \beta a_\Delta) r / r_m$ , leading to the closed loop behavior:

$$\frac{d}{dt} r = -\rho r. \quad (19)$$

In that case, the design parameter  $\rho$  is kept small enough in order not to exceed natural transient rates for which both the original model and the “slowly varying dc component” hypothesis are valid. The maximum allowed stroke is a design constraint and the preceding analysis reveals  $2(\sigma_o - \beta a_\Delta) r / r_m$  as a lower bound. The design considerations above did not relate to the dynamics of  $a_\Delta$ . The rationale is that once both  $r$  and  $r_c$  decay,  $a_\Delta$  will follow, as dictated by (15).

Results are presented here from a simulation with the selection of  $\rho = 0.02$ , and relate to a trajectory that begins at the attractor and terminates near the stabilized steady flow. Figure 4 depicts an actuated transient under closed-loop dynamics of  $a_c$ . From the same figure, the oscillation amplitude can be seen to decrease as control is turned on. A logarithmic scale counterpart of  $\tau$  (not shown) reveals the nearly exponential decay rate, as predicted. The closed-loop dynamics of  $d\phi/dt$  implies a frequency which decreases as one approaches the fixed point. The distance from the fixed point is characterized by

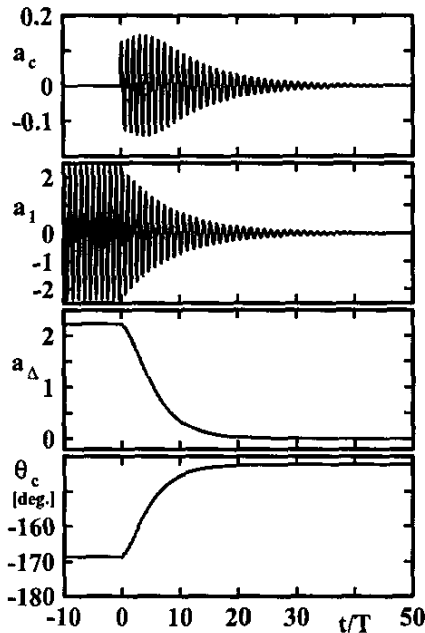


Fig. 4. Transient from natural shedding with a fixed cylinder ( $t < 0$ ) to closed-loop actuation with a moving cylinder ( $t > 0$ ). The time  $t$  is normalized with the period  $T$ . From top to bottom: the actuation amplitude  $a_c$ , the first Fourier coefficient  $a_1$ , the shift-mode amplitude  $a_\Delta$ , and the phase difference  $\theta_c$  in degrees.

$a_\Delta$ . An intriguing result is the change of the phase difference  $\theta_c$  as one approaches the fixed point. The necessity of a varying phase difference to stabilize the near-wake has numerically observed by [3].

Figure 5 shows a phase-space closed-loop dynamics of the state vector  $\mathbf{a}$ .

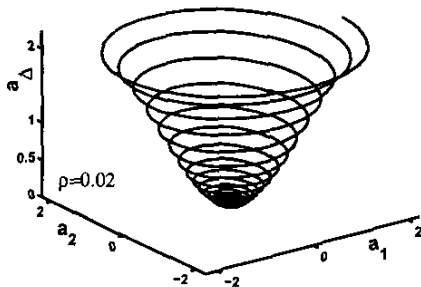


Fig. 5. Phase-space dynamics for the trajectory displayed in Fig. 4.

#### IV. CONCLUSIONS

A novel actuation representation for the empirical Galerkin method has been proposed for imposed flow unsteadiness. Its applicability has been illustrated for vortex shedding behind an oscillating cylinder. This actuation model removes the hardwiring between the Karhunen-Loève modes and the cylinder motion of the reference simulation. In other words, the cylinder motion is a free actuation input in the modified Galerkin system. Thus, the enhanced model enables dissipative control-design for the attenuation of vortex shedding. The

Navier-Stokes simulation with open-loop actuation is well reproduced by that model. For closed-loop attenuation of vortex shedding, a dissipative controller is successfully developed for that model. Recent results show an effective near-wake suppression of vortex shedding due to the described control in the full system, the Navier-Stokes simulation, as will be described in a separate study. For wake control with a volume force [6], similar controllers have reduced the fluctuation level close to the lowest achievable bound in direct numerical simulations.

**Acknowledgments:** The work has been supported by the U.S. National Science Foundation under grants ECS-0136404, CCR-0208791 and INT INT-0230489, by the DAAD program (PPP USA), by the Deutsche Forschungsgemeinschaft (DFG) under grant NO 258/1-1, and by the DFG via the Collaborative Research Center (Sfb 557) "Control of complex turbulent shear flows" at the Technical University of Berlin.

#### REFERENCES

- [1] P. HOLMES, J. L. LUMLEY & G. BERKOOZ 1998 *Turbulence, Coherent Structures, Dynamical Systems and Symmetry*, Cambridge University Press, Cambridge.
- [2] E. DETEMPLE-LAAKE & H. ECKELMANN 1989 Phenomenology of Kármán vortex streets in oscillatory flow. *Exps. Fluids* 7, 217–227.
- [3] S. SIEGEL, K. COHEN & T. MCLAUGHLIN 2003 Feedback Control of a Circular Cylinder Wake in Experiment and Simulation, *AIAA-Paper 2003-3571*, 33rd AIAA Fluids Conference and Exhibit.
- [4] C. MIN & H. CHOI 1999 Suboptimal feedback control of vortex shedding at low Reynolds numbers, *J. Fluid Mech.* 401, 123–156.
- [5] Z. LI, I.M. NAVON, M.Y. HUSSAINI & F.X. LE DIMET 2003 Optimal control of cylinder wakes via suction and blowing, *Computers & Fluids* 32, 149–171.
- [6] J. GERHARD, M. PASTOOR, R. KING, B. R. NOACK, A. DILLMANN, M. MORZYŃSKI & G. TADMOR 2003 Model-based control of vortex shedding using low-dimensional Galerkin models, *AIAA-Paper 2003-4261*, 33rd AIAA Fluid Dynamics Conference and Exhibit.
- [7] P. BLOSSEY, & J. LUMLEY 1998 Control of turbulence, *Ann. Rev. Fluid Mech.* 30, 311–327.
- [8] O. REDINIOTIS, J. KO, & A. KURDILA 2002 Reduced order nonlinear Navier-Stokes models for synthetic jets. *J. Fluids Enrg.* 124, 433–443.
- [9] B.R. NOACK, K. AFANASIEV, M. MORZYŃSKI, G. TADMOR & F. THIELE 2003 A hierarchy of low-dimensional models for the transient and post-transient cylinder wake, *J. Fluid Mech.* 497, 335–363.
- [10] D. REMPFER 1991 *Kohärente Strukturen und Chaos beim laminar-turbulenten Grenzschichtumschlag* (transl.: Coherent structures and chaos of the laminar-turbulent boundary-layer transition), PhD thesis, Fakultät Verfahrenstechnik der Universität Stuttgart (Part of this work has been published by D. REMPFER, & F.H. FAZLE 1994 in *J. Fluid Mech.* 260 & 275).
- [11] B.R. NOACK, P. PAPAS, & P.A. MONKEWITZ 2002 Low-dimensional Galerkin model of a laminar shear-layer. *Tech. Rep.* 2002-01. Laboratoire de Mécanique des Fluides, Département de Génie Mécanique, Ecole Polytechnique Fédérale de Lausanne, Switzerland (Part of the work has been submitted by the same authors as *J. Fluid Mech.* manuscript).
- [12] B.R. NOACK & H. ECKELMANN 1994 A low-dimensional Galerkin method for the three-dimensional flow around a circular cylinder. *Phys. Fluids* 6, 124–143.
- [13] C.H.K. WILLIAMSON 1996 Vortex dynamics in the cylinder wake, *Annu. Rev. Fluid Mech.* 28, 477–539.
- [14] M. MORZYŃSKI, K. AFANASIEV & F. THIELE 1999 Solution of the eigenvalue problems resulting from global non-parallel flow stability analysis, *Comput. Meth. Appl. Mech. Engrg.* 169, 161–176.
- [15] A.E. DEANE, I.G. KEVREKIDIS, G.E. KARNIADAKIS & S.A. ORSZAG 1991 Low-dimensional models for complex geometry flows: Application to grooved channels and circular cylinders, *Phys. Fluids A* 3, 2337–2354.
- [16] G. TADMOR & B.R. NOACK 2004 Dynamic estimation for reduced Galerkin models of fluid flows, to appear in *Proceedings of the 2004 American Control Conference*.
- [17] G. TADMOR, B.R. NOACK, A. DILLMANN, J. GERHARD, M. PASTOOR, R. KING & M. MORZYŃSKI 2003 Control, observation and energy regulation of wake flow instabilities, Paper WEM10-4, *Proceedings of 42nd IEEE Conference on Decision and Control* 2003.